Wang *et al. Annals of Microbiology* (2022) 72:1
https://doi.org/10.1186/s13213-021-01656-2

Annals of Microbiology

UNIVERSITÀ DEGLI STUDI DI MILANO

ORIGINAL ARTICLE

Open Access

Prospecting the plant growth–promoting activities of endophytic bacteria *Franconibacter* sp. YSD YN2 isolated from *Cyperus esculentus* L. var. sativus leaves

Saisai Wang[1†], Jinbin Wang[2,3†], Yifan Zhou[2,3], Yanna Huang[2,3*] and Xueming Tang[1,2,4*]

Abstract

Purpose: Plant growth–promoting (PGP) bacteria are an environment-friendly alternative to chemical fertilizers for promoting plant growth and development. We isolated and characterized a PGP endophyte, YSD YN2, from the leaves of *Cyperus esculentus* L. *var. sativus*.

Methods: Specific PGP characteristics of this strain, such as phosphate solubilization ability, potassium-dissolving ability, siderophore and indole-3-acetic acid (IAA) production, and salt tolerance, were determined in vitro. In addition, positive mutants were screened using the atmospheric and room temperature plasma (ARTP) technology, with IAA level and organic phosphate solubility as indices. Furthermore, the effect of the positive mutant on seed germination, biomass production, and antioxidant abilities of greengrocery seedling was evaluated, and the genome was mined to explore the underlying mechanisms.

Results: The strain YSD YN2 showed a good performance of PGP characteristics, such as the production of indole acetic acid and siderophores, solubilization ability of phosphate, and potassium-dissolving ability. It was recognized through 16S rRNA sequencing together with morphological and physiological tests and confirmed as *Franconibacter* sp. The strain exposed to a mutation time of 125 s by ARTP had the highest IAA and organic phosphate (lecithin) concentrations of 9.25 mg/L and 16.50 mg/L, 50.41% and 30.54% higher than those of the initial strain. Inoculation of mutant strain YSD YN2 significantly increased the seed germination, plant growth attributes, and the activities of peroxidase (POD) and superoxide dismutase (SOD), respectively, but decreased the content of malondialdehyde (MDA) significantly compared with the control. Furthermore, genome annotation and functional analysis were performed through whole-genome sequencing, and PGP-related genes were identified.

Conclusion: Our results indicated that the mutant strain YSD YN2 with PGP characteristics is a potential candidate for the development of biofertilizers.

Keywords: *Cyperus esculentus* L. var. sativus, Atmospheric and room temperature plasma (ARTP), Plant growth–promoting characteristics, Whole-genome sequencing

*Correspondence: yuky8088@163.com; xueming70@foxmail.com
†Saisai Wang and Jinbin Wang contributed equally to this work.
[2] Biotechnology Research Institute Key Laboratory of Agricultural Genetics and Breeding, Shanghai Academy of Agricultural Sciences, Shanghai 201106, China
Full list of author information is available at the end of the article

Introduction

Cyperus esculentus L. var. sativus (*C. esculentus* L.), also referred to as chufas, earth nuts, or tigernut, ranks second in abundance among the Cyperaceae family. *Cyperus* belongs to a genus type in this family, which represents

the 'core taxon' in the family (Huygh et al. 2010; Larridon et al. 2011). Recent studies have illustrated that *C. esculentus* L. is precious for the high-quality oils similar to olive oil, rich in ingredients, and useful parts within the leaf samples like flavonoid, lactones, coumarins and their glycosides, steroids and triterpenoids, and cardiac glycosides (Nyarko et al. 2011; Bado et al. 2015; Ntukidem et al. 2019). They mostly possess the pharmaceutical activities including antioxidant, antimicrobial, and anticoagulating activities, as well as the ability of *C. esculentus* L. to improve blood microcirculation and prevent ischemic stroke (Jing et al. 2016; Jing et al. 2020).

Plant growth–promoting (PGP) bacteria exert plant growth promotion and/or biocontrol effects and are found in the rhizosphere, plant surface, as well as inside the tissues. These PGP bacteria can improve the extent or quality of plant growth directly by increasing nutrient cycling, such as biological nitrogen fixation, solubilization of phosphorus, siderophore production, synthesis of phytohormones, and so on. The use of PGP bacteria is steadily increasing in agriculture as nutrient supplements to soil or the plant, which offer an alternative to chemical fertilizers, antibiotics, herbicides, and pesticides (Calvo et al. 2014). Thus, the use of microbial agents is a promising alternative in environment-friendly agriculture (Vinale et al. 2007; Santoyo et al. 2016).

The endophytes, as an important source of PGP bacteria, are a kind of microbiota that colonize and inhabit internal plant tissues without causing any apparent damage (Strobel et al. 1993). These bacteria exert multiple beneficiary effects, including direct stimulation of plant growth by the action of phytohormones or the production of metabolites within the plant. Beneficial endophytes can produce a number of compounds which are useful for enhancing plant growth and sustainability, while living conveniently inside the hosts (Kang et al. 2014; Ryu et al. 2003; Wilson et al. 2006; Morales-Cedeño et al. 2021). However, the roles of endophytes in plant growth promotion and their behavior in *C. esculentus* L. have not been well studied. Atmospheric and room temperature plasma (ARTP) is a potent mutagenesis tool to induce biological mutation which has succeeded in obtaining strains with desirable characteristics among bacteria, fungi, and microalgae in recent years. It can cause damage to the DNA and induce biological cells to initiate ROS repair mechanisms at room temperatures under atmospheric pressure. Nowadays, ARTP has been proven to be an effective method to generate stable high-yield mutant strains for microorganism breeding (Yang et al. 2019; Gao et al. 2020; Shu et al. 2020; Ottenheim et al. 2018).

In this study, the microbial endophytes of *C. esculentus* L. were isolated, and its PGP characteristics was determined, such as phosphate solubilization ability, potassium-dissolving ability, siderophore and indole-3-acetic acid (IAA) production, and salt tolerance properties. Positive mutants were screened as the candidate of microbial agents through ARTP technology by using IAA level and phosphorus solubility as indices. In addition, the effect of the excellent mutation on seed germination, biomass production, and antioxidant activities of greengrocery plants was determined to evaluate the PGP performance. Furthermore, to fully understand the underlying PGP mechanisms, the genome of the strain YSD YN2 was also analyzed.

Materials and methods

Isolation and identification of endophytic bacteria

Endophytic bacterium YSD YN2 was isolated from *C. esculentus* L. leaves according to the method described by Chen et al. (2019). Briefly, C. *esculentus* L. leaves were surface-sterilized by immersion in 75% ethanol for 3 min, 3% sodium hypochlorite for 6 min, and 75% ethanol for 30 s, then rinsed six times with sterile distilled water. The effect of surface sterilization was checked by spreading the final rinse water (200 μL) onto Luria-Bertani (LB) plates and culturing at 37 °C for 48 h. Sterilized leaves were further mashed aseptically with 5 mL PBS buffer, and the obtained sample was diluted and plated onto LB plates for culture 48 h. Different colonies were selected and streaked on LB plates to check the purity.

To identify the endophytic bacterium, morphological, physiological, and molecular characterization of strain YSD YN2 were analyzed. Briefly, morphological characteristics of bacterial cells were examined using light microscopy; morphological characteristics of bacterial colonies were directly observed, and physiological characteristics of strain YSD YN2 including methyl red (MR) test, Voges–Proskauer (VP) test, catalase activity, starch hydrolysis, citrate utilization, aerobic test, carbon utilization (maltose, sucrose, and glucose), and nitrogen utilization (ammonium sulfate and ammonium nitrate) were determined by standard methods (Wang et al. 2018). Molecular characterization was performed by 16S rDNA sequencing according to the method of Nanjundan et al. (2019). A phylogenetic tree was constructed using the neighbor-joining method of MEGA 7.0 (Tamura et al. 2013).

Plant growth–promoting properties

Phosphate solubilization

The qualitative estimation of phosphate solubilization was performed as per standard method (Mukhtar et al. 2017). Briefly, 24-h cultured bacteria were streaked onto the Pikovskayas medium amended with organic phosphate (lecithin: 0.2 mg/mL) and inorganic

phosphate ($Ca_3(PO_4)_2$: 5 mg/mL) and incubated at 30 °C for 4–5 days. Appearance of a clear halo zone around the bacterial colony indicated phosphate solubilization. For quantitative analysis, the chlorostannous-reduced molybdophosphoric acid blue method was used to analyze phosphate solubilization. Briefly, the 5-mL bacterial culture grown in the Pikovskayas medium amended with soluble and insoluble phosphate was centrifuged at 10,000 rpm for 10 min, and the aqueous phase was collected. To the 1 mL aqueous phase, 10 mL chloromolybdic acid was added, and the final volume was made to 40 mL by the addition of distilled water. The amount of phosphate solubilization was measured at 720 nm using a UV–Vis spectrophotometer. The amount of phosphate solubilization was determined using potassium di-hydrogen phosphate (0–1 µg/mL) as the standard curve.

Siderophore production

The production of siderophore was analyzed as described by Schwyn and Neilands (1987). The isolate was cultured in beef extract peptone liquid medium for 14 h. Five microliters of bacterial liquid was inoculated to CAS plate for 2–3 days at 30 °C; the strain producing orange iron chelating circle was further detected. The isolate was inoculated into the MKB culture medium at 30 °C for 2 days. After incubation, the culture was centrifuged for 10 min at 10,000 rpm; the same volume of supernatant was mixed with CAS detection solution and reacted for 20 min. The absorbance was determined at 630 nm (i.e., As). The same volume of MKB medium and CAS detection solution were used as control, and the absorbance was determined at 630 nm, that is, Ar. According to the formula $\left(\frac{As-Ar}{Ar}\right) \times 100\%$, the amount of iron carrier was calculated.

Potassium solubilization

The K-solubilizing ability of isolates was analyzed with Aleksandrov agar medium (Yaghoubi Khanghahi et al. 2018). Briefly, the isolates were screened by culturing at 30 °C for 4–5 days. Obvious potassium releasing circle appeared, which proved that the isolates had the ability of potassium solubilization. K solubilization efficiency (KE) was calculated by the Ramesh et al. (2014) method.

$$KE = \big(\big(\text{Diameter of solubilization halo zone} + \text{Diameter of colony}\big)/\big(\text{Diameter of colony}\big)\big).$$

Indole-3-acetic acid production

Indole-3-acetic acid (IAA) production was determined by the method described by Ahmad et al. (2008) with some modifications. Briefly, the bacterial culture was inoculated in the Luria broth amended by L-tryptophan (0.1 mg/mL) and incubated at 37 °C for 5 days. After incubation, the culture was centrifuged for 10 min at 6000 rpm. To the 2 mL supernatant, two drops of orthophosphoric acid and 2 mL Salkowski's reagent (50 mL 35% perchloric acid; 1 mL 0.5 $FeCl_3$) were mixed and incubated for 30 min in dark at room temperature. The density of red color was measured by a spectrophotometer with wavelength 530 nm. Value was calculated from the standard graph of IAA (concentration 10–100 mg/L).

Salt tolerance assay

The log phase culture of YSD YN2 (OD_{600} = 0.1) was added to Luria broth amended with different concentrations of NaCl (1, 2, 4, 6, 8, and 10% w:v) and incubated for 56 h at 37 °C (180 rpm). Samples were drawn after every 4 h, and optical density was measured (at 600 nm) using Thermo Scientific^{TM} Evolution 201 UV–Vis spectrophotometer up to stationary phase (Hmaeid et al. 2019). The experiment was conducted in triplicates.

Procedures for ARTP mutagenesis

The YSD YN2 strain was mutated through the ARTP technology according to a previously described method (Zhuang et al. 2020; Fan et al. 2017). The mature bacterial suspension grown on LB medium was washed with 0.85% sterile saline solution and then diluted to an OD_{600} of 0.6–0.8 before mutagenesis. Next, 10 µL of the bacterial suspension was spread on steel plate and subjected to ARTP (Wuxi TMAXTREE Biotechnology Co., Ltd., China) irradiation for different mutation times (0 s, 25 s, 50 s, 75 s, 100 s, 125 s) at a radio frequency power input of 100 W and helium gas flow of 10 L/min. The steel plates with treated bacteria were transferred into the centrifuge tubes containing 1 mL sterile distilled water. The treated bacteria were diluted and coated onto an LB plate. The lethal rate was calculated by plate colony count and untreated samples as control.

$$\text{Lethal rate}\,(\%) = \frac{\text{Number of colonies without mutation treatment} - \text{Number of colonies treated by mutation}}{\text{Number of colonies without mutation treatment}} \times 100$$

Mutant colonies were randomly picked up and inoculated into the fermentation medium in shaking flasks for evaluation of IAA production and phosphate solubilization. Hereditary stability of the mutant strain was studied. Finally, the ability of the mutant strain to produce IAA was further checked by using Salkowski's reagent with L-tryptophan at different concentrations (1 mg/mL, 2 mg/mL, and 5 mg/mL) and without L-tryptophan

through colorimetry, as described previously (Shi et al. 2018).

Seed germination

Seeds of greengrocery were surface-sterilized with 1% (w/v) mercuric chloride followed by 75% (v/v) ethanol. Seeds were thoroughly rinsed with deionized water and allowed to imbibe for 3 h. After imbibition, the seeds were placed into Petri plates containing sterile filter sheets moistened with either 2 mL of distilled water (these controls were labeled as "control") or a different concentration of the mutant strain YSD YN2 (2×10^7, 2×10^6, and 2×10^5 CFU/mL) and cultured at 25 °C. The number of germinated seeds was counted at 48-h intervals for 10 days. Germination rate (%) $= \frac{\text{Number of germinating seeds}}{\text{Total number of tested seeds}} \times 100$. The experimental treatments were conducted in 3 replications, in which there were 20 seeds per replicated unit.

Role of endophytic inoculation in plant development

Greengrocery was grown within a greenhouse at 25–30 °C with tap water irrigation in the absence of any fertilizer at the Shanghai YuanJu Food, Fruit, and Vegetable Cooperative (121° 15′ 23″ E, 31° 26′ 7″ N), Shanghai, China. The field soil was black and calcareous; the total nitrogen level was 2.19 g/kg; available nitrogen level was 152.55 g/kg; organic matter content was 23.58 g/kg; available phosphorus level was 90.30 mg/kg; total phosphorus level was 1.54 g/kg; total potassium level was 17.04 g/kg, and available potassium level was 360.23 mg/kg. The greengrocery cultivar huawang was used for the experiment that was performed on 1 October, 2020. In the 2nd and 4th weeks after sowing, the mutant strain YSD YN2 at a concentration of 10^6 CFU/mL was sprayed evenly on the seedlings, and water was used as the control. After 42 days, greengrocery was harvested, and the plant height, root length, and number of leaves were measured simultaneously. After separating the roots and shoots, roots were rinsed with tap water to remove soil particles. Thereafter, plant growth attributes, such as root diameter, biomass, vitamin B1, vitamin C, and chlorophyll content were determined, and dry biomass of the plant that was dried in an oven at 65 °C until a constant weight was achieved.

Analysis of antioxidant activity in greengrocery leaves

Antioxidant abilities such as malondialdehyde (MDA) content, activity of superoxide dismutase (SOD), and peroxidase (POD) were determined according to previously described methods (Ullah et al. 2017).

Briefly, MDA contents were assessed by grinding 0.5 g of fresh leaves using mortar and pestle in 5 mL 1% trichloroacetic acid (TCA). The resultant supernatant (4 mL) was combined with a solution (4 mL) 20% TCA and 0.5% 2-thiobarbituric acid, then boiled for 30 min, cooled in ice, and centrifuged at 4000 rpm for 10 min. Optical density of the supernatant was measured at 532 nm. The lipid peroxidation level was expressed in micromoles of MDA formed per gram leaf tissue.

SOD activities were assessed by grinding 0.5 g of fresh leaves using liquid nitrogen and extracted in 2 mL of 50 mM phosphate buffer (pH 7.8). The crushed powder was used to determine the SOD activities. The protein contents were determined through the Bradford assay using bovine serum albumin as a standard (Bradford 1976). The SOD activity was assessed based on superoxide inhibition of NBT reduction. The activity was calculated through the standard curve at 560 nm.

For POD activity, firstly, samples were ground in liquid nitrogen, and 0.1 mL powder was suspended in extraction buffer (0.1 M phosphate buffer (pH 6.8), 50 µL pyrogallol). Secondly, 50 µL of H_2O_2 was added, and the mixture was incubated at 30 °C for 5 min. The reaction was stopped with the addition of 5% H_2SO_4 (v/v). POD activities were measured at 420 nm in a spectrophotometer. Activity was expressed as a 0.1 unit increase in enzyme absorbance.

Genome sequencing, assembly, and annotation

The mutant strain YSD YN2 was cultured in LB at 37 °C for 24 h, then genomic DNA was extracted using a bacterial genomic DNA extraction kit. Then, a 10-kb insert SMRTbell DNA library was constructed and sequenced on the single-molecule real-time (SMRT) sequencing platform using the PacBio RS II sequencer (Faino et al. 2015). Subsequently, a high-quality dataset was constructed, and the related sequencing depth was 100-fold.

A de novo paired-end read assembly was created using SOAPdenovo2 (Luo et al. 2012), whereas Canu and SPAdes were used to assemble an integrated genomic map of the mutant strain YSD YN2 genome (Bankevich et al. 2012). In addition, GeneMarkS (Besemer and Borodovsky 2005) and Glimmer (Delcher et al. 2007) were used for predicting plasmid-related genes and coding sequences (CDSs), respectively. tRNA and rRNA genes were predicted using tRNAscan-SE v. 2.0 and Barrnap v. 0.8, respectively (Chan and Lowe 2019). Prophages were predicted using PHage Search Tool (Bertelli et al. 2017). IslanderViewer v. 1.2 (Fouts 2006) was used to predict gene island (GI). We acquired other annotations based on databases, namely Gene Ontology (GO), Kyoto Encyclopedia of Genes and Genomes (KEGG; Kanehisa and Goto 2000), Clusters of Orthologous Group (COG; Jensen et al. 2008), Non-Redundant Protein (NR), Swiss-Prot (Bairoch and Apweiler 2000), and Pfam (Finn et al. 2014), through BLASTp at identical BLAST thresholds.

Table 3 exhibits fundamental genome sequencing results of mutant strain YSD YN2. By using sequence alignment tools such as HMMER v. 3.1b2, Diamond v. 0.8.35, and BLAST v. 2.3.0 + (Cai et al. 2018), carbohydrate-active enzymes (CAZy) based on pathogen–host interactions (PHI) and comprehensive antibiotic resistance database (CARD) were analyzed. Clustered Regularly Interspersed Short Palindromic Repeats-Cas (CRISPR-Cas) genes were predicted by using Minced (Bland et al. 2007). AntiSMASH v. 4.0.2 was used to predict gene clusters of secondary metabolites (Blin et al. 2017).

Statistical analysis

Mean and standard deviations were calculated through the analysis of variance (ANOVA) at a level of 5% by using PSS 19.0 (IBM SPSS Statistics 19, USA).

Results and discussion

Strain identification

Morphological observation showed the YSD YN2 strain was rod shaped and Gram negative, and colonies growing on LB agar medium were opaque, rough, and creamy white colonies with irregular edge. Physiologically, strain YSD YN2 can utilize glucose, sucrose, maltose, ammonium sulfate, and ammonium nitrate; showed production of catalase and citrate; and was positive for methyl red (MR) test, starch hydrolysis, and nitrogenase but negative for Voges–Proskauer (VP) test and aerobic test (Table 1). Furthermore, the 16S rRNA sequence of strain YSD YN2 (GenBank accession number OK103794) showed 99% similarity with *Franconibacter helveticus* strain Z96 (GenBank accession number KF835772). And the neighbor-joining tree also showed strain YSD YN2 phylogenetic clustering with validly published type species obtained from a database of species type *Siccibacter zurichensis* strain Z22 (GenBank accession number KF835735) in the NCBI database (Fig. 1). Hence, it was confirmed that YSD YN2 belongs to the *Franconibacter* sp.

Plant growth–promoting properties and salt tolerance

Qualitative and quantitative analysis of PGP properties confirmed YSD YN2 as IAA and siderophore producer along with the ability to solubilize P and K (Table 1). YSD YN2 was found to have K solubilization efficiency of 2.38 ± 0.056 and siderophore production of 0.20 ± 0.005%. The IAA yields of YSD YN2 without L-tryptophan and with 0.1 mg/mL L-tryptophan were 6.15 ± 0.068 and 9.00 ± 0.012 mg/L, respectively. The phosphate solubilization of YSD YN2 to organic phosphate (lecithin) was stronger than that of inorganic phosphate ($Ca_3(PO_4)_2$); the quantitative estimation of phosphate solubilization were 2.64 ± 0.452 and 1.24 ± 0.024 mg/L, respectively. The salinity tolerance assay showed that 6% NaCl did not significantly affect the growth of

Table 1 Biochemical and functional characterization (plant growth–promoting activities) of YSD YN2

			YSD YN2
Biochemical attributes	Gram stain		-
	Catalase test		+
	Methyl red test		+
	Voges-Proskauer test		-
	Citrate test		+
	Starch hydrolysis test		+
	Aerobic test		-
	Carbon source	Glucose	+
		Sucrose	+
		Maltose	+
	Nitrogen source	Ammonium sulfate	+
		Ammonium nitrate	+
	Phosphate solubilization	Lecithin (D/d)	3.05 ± 0.045
		$Ca_3 (PO_4)_2$ (D/d)	-
		Lecithin (mg/L)	12.64 ± 0.452
		$Ca_3 (PO_4)_2$ (mg/L)	1.24 ± 0.024
	Siderophore production (%)		0.20 ± 0.005
	K solubilization efficiency (KE)		2.38 ± 0.056

Note: (+) positive reaction; (-) negative reaction. Results are means ± SD ($n = 3$) of three independent experiments with each treatment measured on three repetitions. *D/d*, transparent zone diameter/ colony diameter

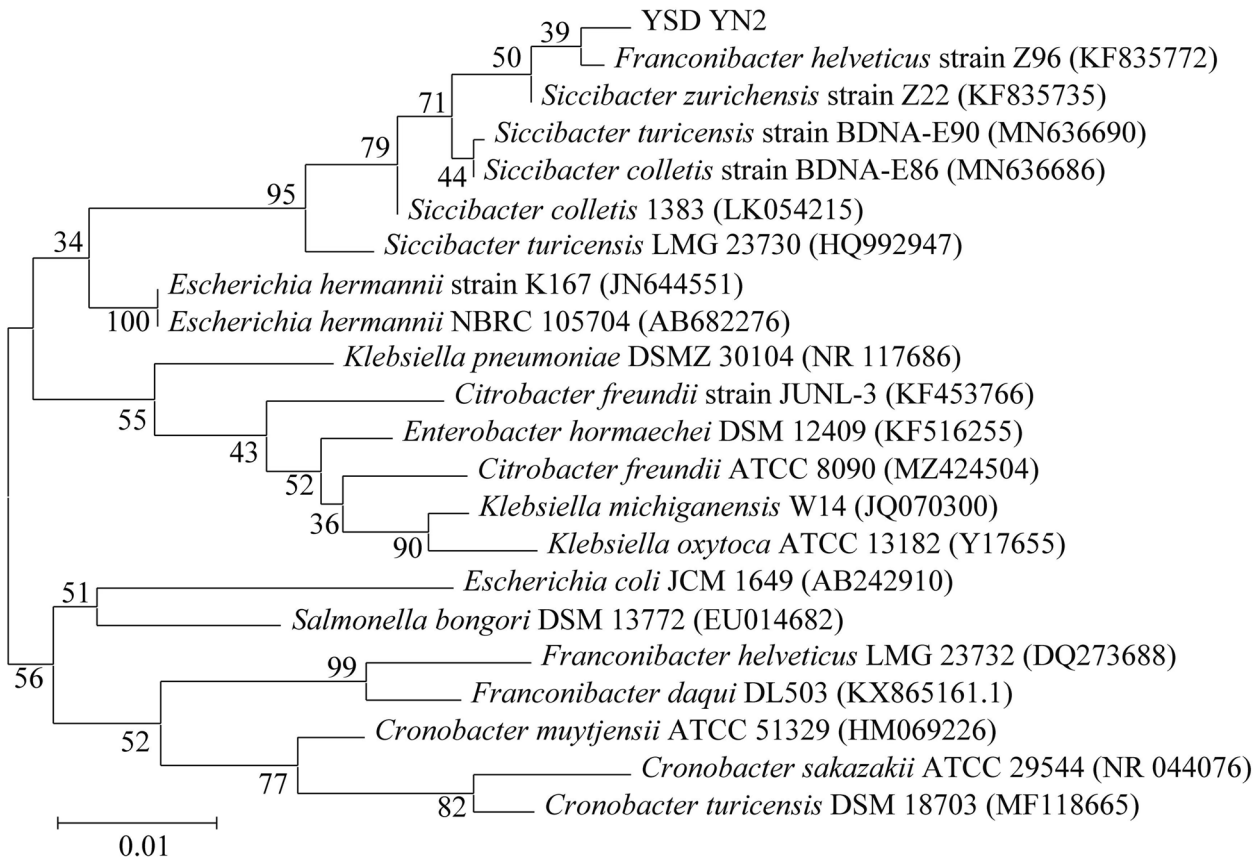

Fig. 1 Phylogenetic tree of the strain YSD YN2 based on 16S rDNA gene sequence

YSD YN2. However, further increase in salt concentration reduced the tolerance and survival rate of bacteria (Fig. 2).

Strain improvement and screening through ARTP

As shown in Fig. 3a, when ARTP mutagenic time was increased from 50 to 125 s, the lethal rate of the strain increased from 75.67 ± 2.08%to 89.67 ± 1.00%.When the death rate of ARTP mutation is close to 80%, the positive mutation rate of a strain is higher (Tang et al. 2009). Therefore, 50 s, 75 s, 100 s, and 125 s were considered the ARTP mutation times. As shown in Fig. 3b, although the IAA and organic phosphate concentrations of YSD YN2 with a mutation time of 50 s mildly decreased compared with those of the initial strain, the strains exposed to other mutation times had increased concentrations compared with the initial strain. The strain exposed to a mutation time of 125 s had the highest IAA and organic phosphate concentrations of 9.25 mg/L and 16.50 mg/L, respectively. After culturing for 8 passages (Fig. 3c), IAA and organic phosphate concentrations in the mutant strain reached 9.25 mg/L and 16.50 mg/L, respectively. These values were 50.41% and 30.54% higher than those of the initial strain, suggesting excellent hereditary stability of the mutant strain. As shown in Fig. 3d, YSD YN2 was also tested for its ability to produce IAA in the presence and absence of L-tryptophan. As L-tryptophan concentration increased, the IAA production increased significantly; YSD YN2 produced the largest amount of IAA (16.51 ± 0.558 mg/L) at the concentration of L-tryptophan of 5 mg/L. There were highly significant differences for YSD YN2 in terms of the presence and absence of L-tryptophan ($P < 0.0001$). Therefore, the strain with the 125-s mutation time was selected for further analyses.

Effects of different concentrations of strain on seed germination

Three concentrations of mutant strain YSD YN2 were selected based on their potential PGP properties. The results revealed that with an increase in the time beyond the third day, the germination rate of seeds in each treatment increased, and the germination rate tended to be stable from the seventh day (Fig. 4). Analysis of variance indicated that germination rate of the seeds

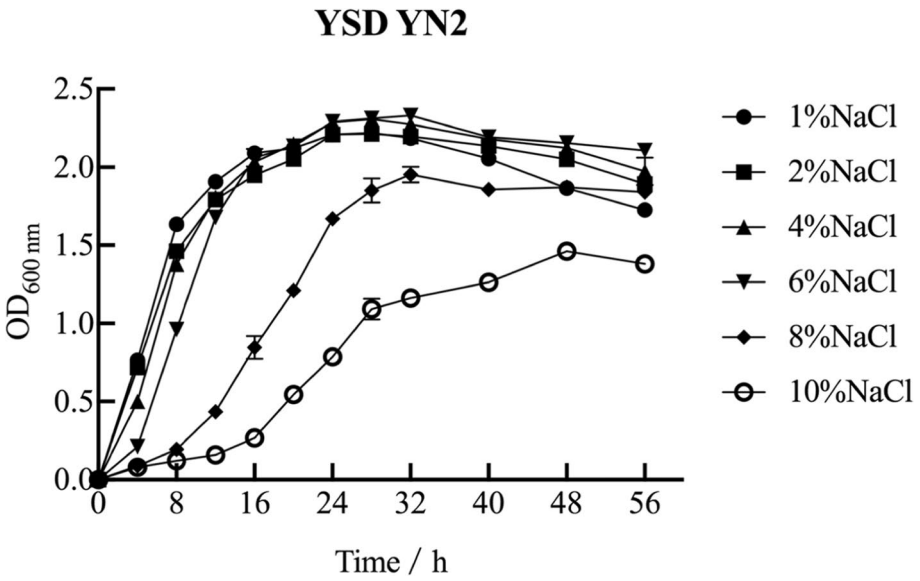

Fig. 2 Salinity tolerance growth curve of YSD YN2 under various saline conditions (1-10% NaCl). Error bars show the standard deviation of the mean values of three replicates

incubated with the mutant strain YSD YN2 at 2×10^6 CFU/mL were significantly ($P < 0.0001$) increased compared with the control. However, compared with the control, the germination rate of seeds incubated with the mutant strain YSD YN2 at 2×10^7 CFU/mL and 2×10^5 CFU/mL decreased, but there was no significant difference with the control. Rowse (1995) reported that incubated seeds rapidly imbibe and revive the seed metabolism, resulting in a higher germination percentage. The present study supports the earlier findings that seed priming increases percent germination (Kaya et al. 2006). The results indicated that seed incubation with the mutant strain YSD YN2 at 2×10^6 CFU/mL was more effective than the other treatments concerning seed germination.

Effects of the strain on plant biomass and antioxidant activities

Plant growth attributes such as root and shoot length, fresh and dry biomass, vitamin B1, vitamin C, and chlorophyll contents are prime parameters for the assessment of incubation of the isolate. As shown in Table 2, the YSD YN2 mutant strain inoculation significantly increased ($P < 0.05$) the shoot fresh weight, shoot dry weight, root fresh weight, root dry weight, root diameter, leaf number, and vitamin C contents of the shoot by 84.49%, 107.74%, 146.42%%, 138.84%, 85.71%, 37.50%, 33.79%, respectively, compared with those of controls without inoculation, which indicate that the mutant strain YSD YN2 promoted the growth of plant seedlings. Fresh and dry weight increase in response to bacterial inoculation could be due to higher nutrient uptake and enhanced hormone and vitamin production (Delshadi et al. 2017). Similar results were also reported by Bidabadi and Mehralian (2020) concerning the enhanced biomass production of *Dracocephalum Kotschyi* Boiss inoculated with growth-promoting bacteria. Although there was no significant increase in root length, plant height, and vitamin B1 content after greengrocery plants had been treated with the mutant strain YSD YN2, the chlorophyll content was significantly enhanced after treatment, and the mutant strain YSD YN2 effectively stimulated chlorophyll synthesis in greengrocery leaves (Table 2). The genus *Cronobacter* has been previously reported with chlorophyll production ability. Afridi et al. (2019) found chlorophyll production of Pasban 90 of 44.65 ± 0.68 μg/mL and of Khirman of 44.31 ± 0.65 μg/mL. The positive effect of seed bio-priming on the improvement of chlorophyll and plant biomass production may be due to the entrance or adherence of bacteria to the seeds and also acclimatization of bacteria in a permanent condition (Mahmood et al. 2016).

Antioxidants are one of the indicators of a plant's tolerance to stresses (Pan et al. 2013; Esfahani 2011). POD and SOD are the main antioxidant enzymes in plants; their changes can reflect the stress resistance of plants (He et al. 2011). The enzymes of plants coordinate with each other under normal conditions, and the enzyme activity in the defense system becomes the decisive factor to control injury, which can also

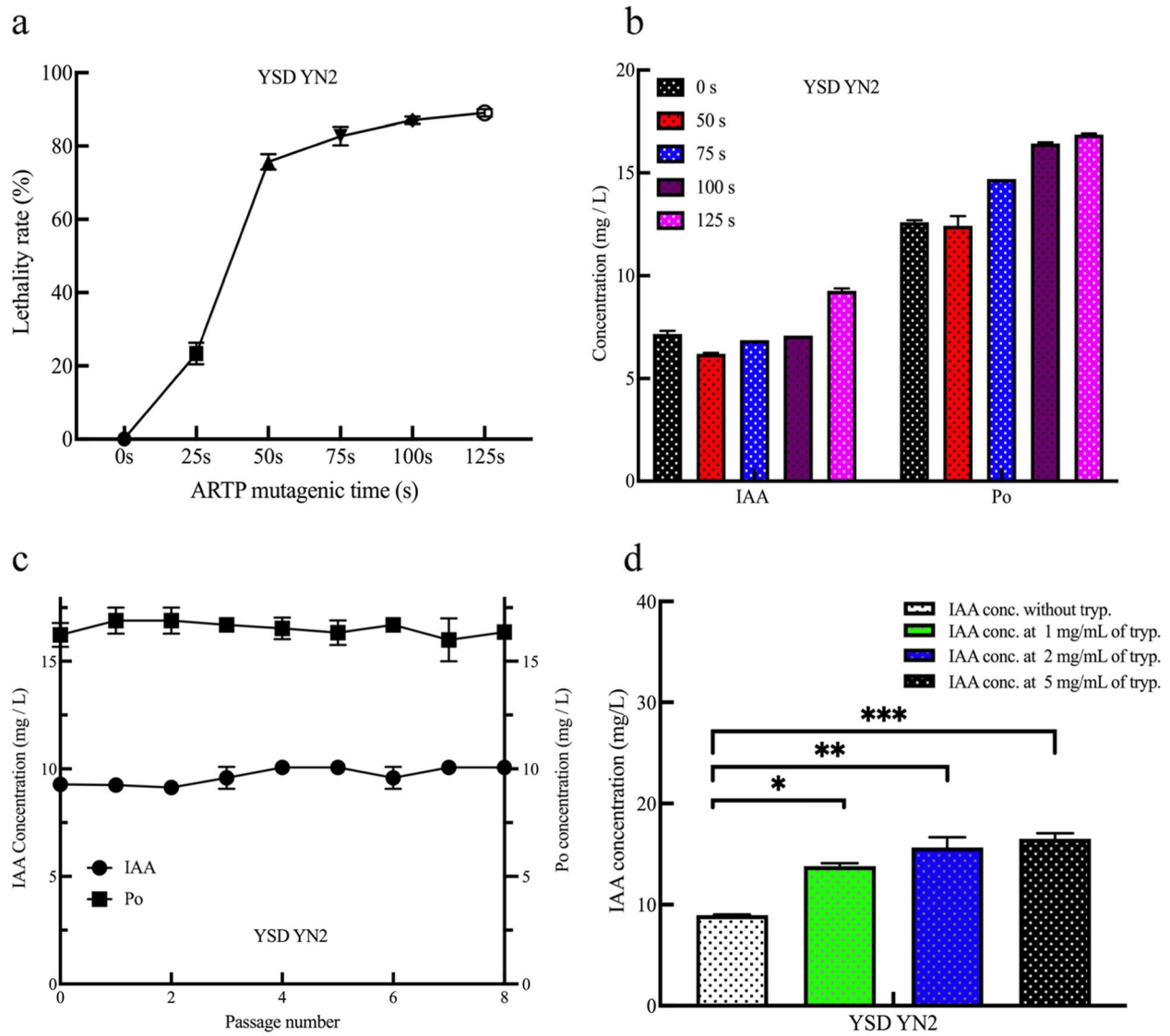

Fig. 3 Strain improvement and screening by ARTP. **a** Lethality rate of YSD YN2 under different mutagenic time. **b** The IAA concentration and organic phosphate concentration (Po) under different mutagenic time. **c** Hereditary stability of mutant strain. **d** Quantitative production of IAA by endophytic bacterial isolates; with and without tryptophan. Experiments were performed in triplicate, and the values are represented as mean ± standard deviation. Data are presented as the mean of 3 replicates. Lowercase for different IAA concentrations at the same strains ($P \leq 0.05$, Tukey's multiple-comparison tests)

better reflect the adaptability of plants to adversity. The activities of antioxidants were evaluated in uninoculated and inoculated plants (Table 2). The activity of SOD and POD were observed to be higher when inoculated with the mutant strain YSD YN2 as compared with the uninoculated plants, and lower MDA content was observed in inoculated plant tissues than the uninoculated ones. Overall results showed that inoculation meaningfully promoted plant growth and stress resistance of plants.

Genomic features of the mutant strain YSD YN2

Following the confirmation of the plant growth–promoting ability of the mutant strain YSD YN2, whole-genome sequence analysis of the mutant strain YSD YN2 was performed in order to obtain a reliable taxonomic classification and identify genes or pathways that could potentially contribute to the plant growth–promoting effects. The genome of the mutant strain YSD YN2 was found to consist of two circular contigs (Fig. 5): a single circular chromosome of 4,066,839 bp and a circular plasmid of 41,462

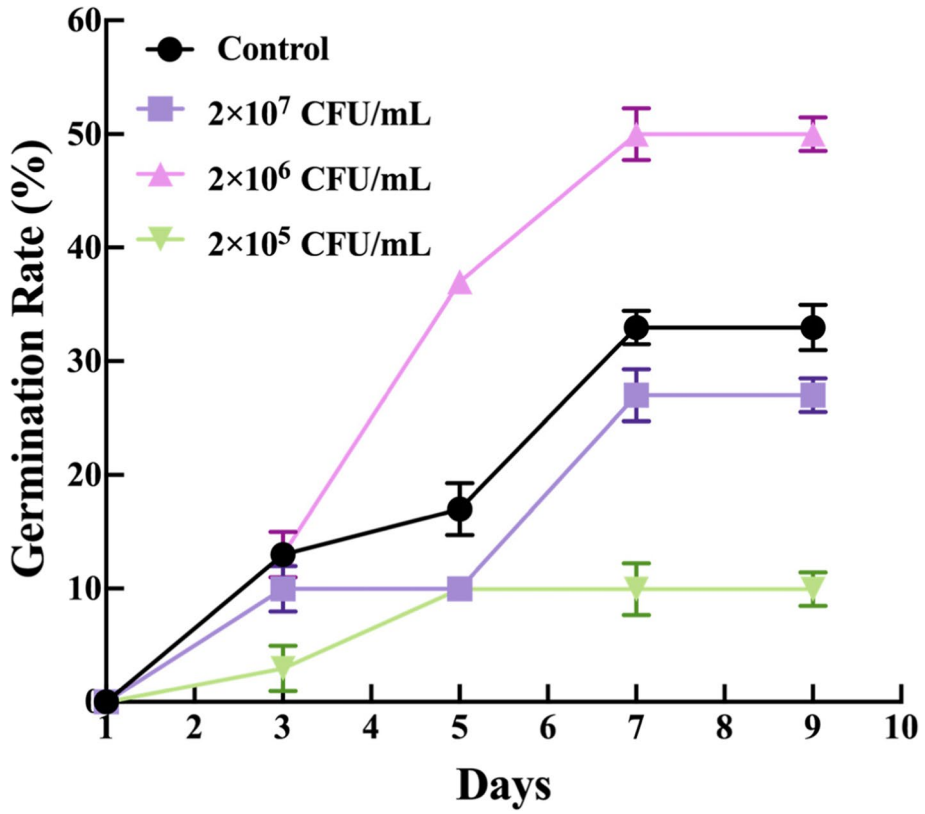

Fig. 4 Seed germination of greengrocery treated with 2×10^7, 2×10^6, 2×10^5 CFU/mL mutant strain YSD YN2. Experiments were performed in triplicate, and the values are represented as mean ± standard deviation. Data are presented as the mean of 3 replicates. Lowercase for different concentrations of strains in the same days ($P \leq 0.05$, Dunnett's multiple-comparison tests)

bp with an average G + C content of 57.45% and 50.24%, respectively (GenBank accession numbers CP074352 and CP074353, respectively). The general characteristics of the mutant strain YSD YN2 genome are summarized in Table 3. Altogether, 3877 protein-encoding genes, 80 tRNAs, 22 rRNAs, 40 repeat DNAs, 4 prophages, 9 GIs, and 7 CRISPR-Cas were predicted in the genome analysis.

Functional analysis of the mutant strain YSD YN2

Of the 3877 protein-encoding genes, we annotated 3526 (90.95%) genes exhibiting specific functions. The numbers of genes annotated from different databases are NR (3877), COGs of proteins (3526), Swiss-Prot (3308), GO (1714), KEGG (2607), Pfam (3436), CAZy (111), PHI (958), CARD (212), and VFDB (514) (Table S1).

According to annotations based on the COG database, 3526 genes were divided into 20 COG categories, many of which were related to functions such as carbohydrate transport and metabolism, amino acid transport and metabolism, transcription, inorganic ion transport and metabolism, and cell wall/membrane/envelope biogenesis (Fig. 6). So far, a few integrated *C. esculentus* L. endophytic bacterial genome sequences have been published. GO annotation suggested that the regulation of transcription and DNA templated showed the highest numbers in terms of biological processes, integral membrane components played an important role in cellular components, and ATP binding played a vital role in molecular function (Figure S1). On the other hand, KEGG annotations revealed that 277 genes were involved in membrane transport, 251 genes participated in carbohydrate metabolism, 170 genes participated in amino acid synthesis, 163 genes participated in the metabolism of cofactors and vitamins, and 145 genes participated in the energy metabolism, indicating that the mutant strain YSD YN2 could perform transmembrane transport and energy substance exchange with the external environment, particularly of proteins related to amino acid and carbohydrate metabolism (Figure S2). The results of annotation also support the speculation that the mutant strain YSD YN2 could produce an iron carrier, synthesize small molecular organic acids and secrete them to dissolve insoluble phosphorus and potassium.

Table 2 Effect of the mutant strain YSD YN2 on plant biomass and antioxidant activities

Treatments	Control	Mutant strain YSD YN2
Plant biomass		
Root length (cm)	5.97 ± 1.66[a]	7.77 ± 0.67[a]
Plant height (cm)	25.17 ± 1.61[a]	30.13 ± 3.18[a]
Leaf number	8.00 ± 1.00[b]	11.00 ± 0.00[a]
Root diameter (mm)	3.43 ± 0.40[b]	6.37 ± 0.67[a]
Fresh weight		
Shoot (g/plant)	28.17 ± 7.09[b]	51.97 ± 2.79[a]
Root (mg)	249.40 ± 63.40[b]	614.57 ± 51.54[a]
Dry weight		
Shoot (g/plant)	4.39 ± 1.11[b]	9.12 ± 0.49[a]
Root (mg)	35.17 ± 10.42[b]	84.00 ± 11.20[a]
Vitamin B1(mg/g)	16.47 ± 0.01[a]	16.97 ± 0.01[a]
Vitamin C(mg/g)	85.94 ± 0.73[b]	114.98 ± 0.57[a]
Chlorophyll content (μg/g)	69.80 ± 7.27[b]	89.67 ± 12.87[a]
Antioxidant activities		
SOD activities ($U \cdot g^{-1}$ $FW \cdot h^{-1}$)	708.99 ± 11.11[b]	761.44 ± 13.82[a]
MDA content (μmol/g)	1.57 ± 0.48[a]	1.29 ± 0.25[b]
POD activities ($U \cdot g^{-1}$ min)	520.00 ± 72.11[a]	566.67 ± 11.55[a]

Note: Values are means ± SD ($n = 3$). Control is non-bacterial inoculated plants. Statistically different from the uninoculated control ($P < 0.05$)

AntiSMASH analysis revealed the presence of 4 clusters of genes for the biosynthesis of secondary metabolites, all of which were present on the chromosome (Table 4). The most interesting are the clusters with high similarity to the biosynthesis of thiopeptide, terpene, and bacteriocin. Many of these compounds may be involved in establishing symbiotic associations with plants (Bélanger et al. 1999; Han et al. 2013). In addition to secondary metabolites, the mutant strain YSD YN2 contains genes involved in CAZy annotation (Table S2) and prediction of VFDB (Table S3), PHI (Table S4), Secretion System (Table S5), CARD (Table S6), and Two components (Table S7).

Genetic factors underlying the promotion of plant growth

Diverse PGP-related genes/gene clusters such as those pertaining to siderophore synthesis, phosphate solubilization and uptake, nutrition utilization, growth-promoting volatile organic compound (VOC) generation, and phytohormone production were identified in the mutant strain YSD YN2 genome through genome mining (Table 5).

Siderophore enterobactin, bacillibactin, and vibriobactin promote plant development and help plants develop pathogenic resistance by forming ion complexes and reducing ion availability to pathogens (Arguelles-Arias et al. 2009). Genes related to siderophore synthetase (entF, entD, entE, entS, entB, entA, and entC) and siderophore transport system (fepA, fepB, fepC, fepD, fepG, fes) were found in the mutant strain YSD YN2 genome. Gluconic acid allows the plants to absorb phosphate and acts by solubilizing poorly soluble minerals, making them available to plants (Stella and Halimi 2015). Gene cluster gcd that encodes glucose-1-dehydrogenase synthetase was found to be present in the mutant strain YSD YN2 genome. Genes related to phosphonate degradation (phnO and pat) were also found in the mutant strain YSD YN2 genome. Two extensively recognized VOCs, namely 2, 3-butendiol and 3-hydroxy-2-butanone, have been suggested to enhance plant development as crop protectants and promote autoimmune function in plants (Fincheira and Quiroz 2018). Moreover, genes associated with 3-hydroxy-2-butanone synthesis namely ketol-acid reductoisomerase (ilvC), acetolactate synthase I/III small subunit (ilvH), acetolactate synthase II small subunit (ilvM), and cetolactate synthase I/II/III large subunit

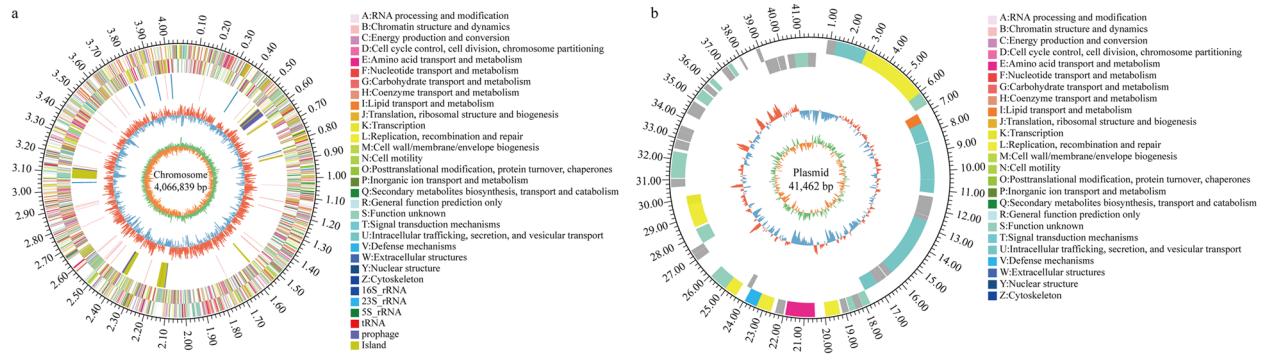

Fig. 5 Circular genome map of mutant strain YSD YN2. **a** chromosome; **b** plasmid. The circular genome map was created using Circos v0.69-6 with COG function annotation. From outside to inside, circle 1, the size of complete genome, each scale represents 20 kb; circles 2 and 3, the predicted protein-coding genes on the + and - strands, different colors represent different COG function classification; circle 4, tRNA, rRNA, prophage and island; circle 5, G + C content, with > 57.45% G + C in red, with ≤ 57.45% G + C in blue; the inner circle, G + C skew, with G% < C% in green, with G% > C% in orange.

Table 3 General features of the mutant strain YSD YN2

Attribute	Value	bp (%) of the genome	GC content (%)
Genome size (bp)	4,108,301	100.00	57.38
Chromosome (bp)	4,066,839	98.99	57.45
Plasmid (bp)	41,462	1.01	50.24
Protein-coding genes	3877	87.11	58.65
Genes assigned to KEGG	2607	-	-
Genes assigned to COG	3526	-	-
Total size of protein-coding genes	3,578,721	-	-
Mean length of protein-coding genes (bp)	923.06	-	-
tRNA number	80	-	-
16S rRNA	7	-	-
23S rRNA	7	-	-
5S rRNA	8	-	-
Repeat DNAs	40	0.36	-
Prophage	4	-	-
GIs	9	-	-
CRISPR-Cas	7	-	-

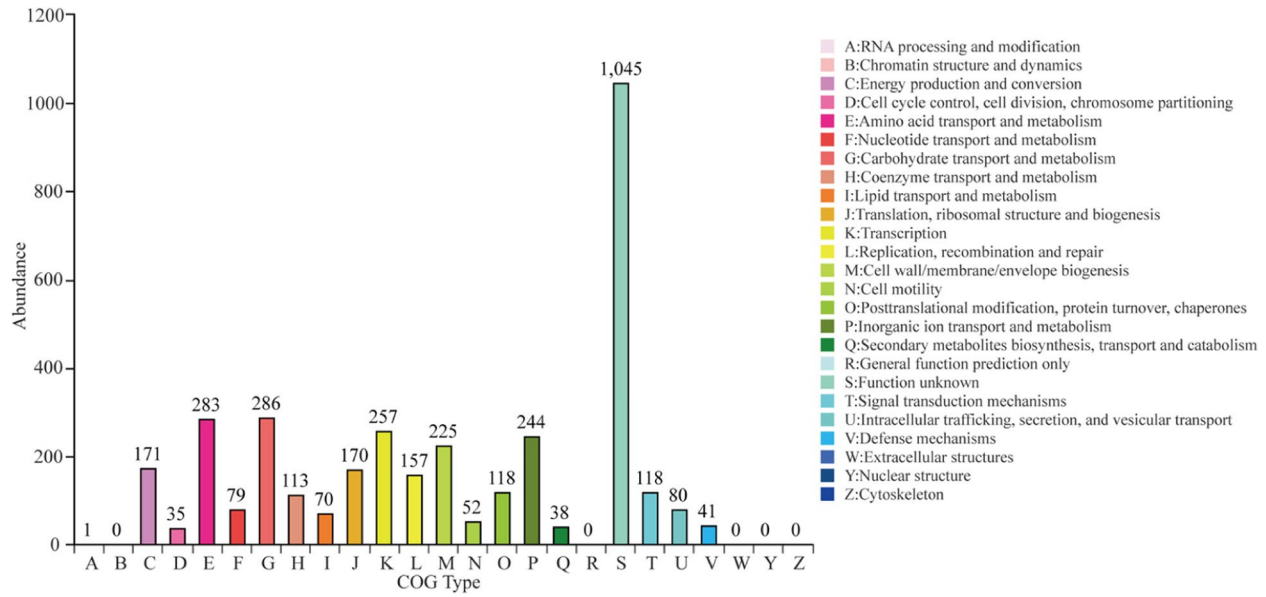

Fig. 6 COG annotation results of mutant strain YSD YN2 genome

Table 4 Putative gene clusters for secondary metabolites identified by AntiSMASH

Location	Chromosome	Chromosome	Chromosome	Chromosome
Cluster ID	Cluster1	Cluster2	Cluster3	Cluster4
Type	NRPS	Thiopeptide	Terpene	Bacteriocin
Start	1,044,236	1,361,711	1,906,337	3,912,804
End	1,096,877	1,388,009	1,929,905	3,923,428
Gene no.	48	23	22	8
Similar cluster	Turnerbactin	O-antigen	carotenoid	-
Similarity (%)	30	14	83	-
Predict core structure	NC(CO)C(=O)O			

Table 5 Genes related to plant growth promotion in the mutant strain YSD YN2 genome

Gene	Gene product	Function
entF	Enterobactin synthetase component F	Siderophore synthesis
entE	2,3-Dihydroxybenzoate-AMP ligase	
entB	Bifunctional isochorismate lyase / aryl carrier protein	
entA	2,3-Dihydro-2,3-dihydroxybenzoate dehydrogenase	
entD	Enterobactin synthetase component D	
entC	Isochorismate synthase	
entS	Enterobactin (siderophore) exporter	
fepA	Ferric enterobactin receptor	
fepC	Ferric enterobactin transport system ATP-binding protein	
fepG	Ferric enterobactin transport system permease protein	
fepD	Ferric enterobactin transport system permease protein	
fepB	Ferric enterobactin transport system substrate-binding protein	
fes	Iron(III)-enterobactin esterase	
gcd	Glucose-1-dehydrogenase	Gluconic acid
pat	Phosphinothricin acetyltransferase	Phosphonates
phnO	(Aminoalkyl)phosphonate N-acetyltransferase	
ilvC	Ketol-acid reductoisomerase	3-Hydroxy-2-butanone synthesis
ilvB	Acetolactate synthase I/II/III large subunit	
ilvM	Acetolactate synthase II small subunit	
ilvH	Acetolactate synthase I/III small subunit	
budC	(S,S)-butanediol dehydrogenase / diacetyl reductase	2,3-Butanediol synthesis
otsA	Trehalose 6-phosphate synthase	Trehalose synthesis
otsB	Trehalose 6-phosphate phosphatase	
treZ	Maltooligosyltrehalose trehalohydrolase	
treA	Alpha,alpha-trehalase	
treC	Trehalose-6-phosphate hydrolase	
speE	Spermidine synthase	Spermidine synthesis
speA	Arginine decarboxylase	
speB	Agmatinase	
speC	Ornithine decarboxylase	
speD	S-adenosylmethionine decarboxylase	
speG	Diamine N-acetyltransferase	
nirD	Nitrite reductase (NADH) small subunit	Nitrogen utilization
narI	Nitrate reductase gamma subunit	
narH	Nitrate reductase / nitrite oxidoreductase, beta subunit	
narG	Nitrate reductase / nitrite oxidoreductase, alpha subunit	
narK	MFS transporter, NNP family, nitrate/nitrite transporter	
nirB	Nitrite reductase (NADH) large subunit	
nrtA	Nitrate/nitrite transport system substrate-binding protein	
nrtB	Nitrate/nitrite transport system permease protein	
nrtC	Nitrate/nitrite transport system ATP-binding protein	
nasA	Assimilatory nitrate reductase catalytic subunit	

(ilvB) have been identified in the genome. We also discovered the gene encoding (S,S)-butanediol dehydrogenase/diacetyl reductase (budC), which is responsible for catalyzing 3-hydroxy-2-butanone into 2, 3-butanediol, in the genome (Table 5). Additionally, phytohormones such as trehalose was found in the genome. Trehalose, a stress-resistant compound, can resist abiotic stresses such as dehydration, high/low temperature, drought, and salinity, and increased levels of trehalose in cells have been shown to enhance host tolerance to stress

(Farías-Rodríguez et al. 1998; Suárez et al. 2008; Brodmann et al. 2002; Isidorov et al. 2008). Genes responsible for the synthesis of trehalose, namely trehalose 6-phosphate synthase (otsA), maltooligosyltrehalose trehalohydrolase (treZ), trehalose 6-phosphate phosphatase (otsB), alpha, alpha-trehalase (treA), and trehalose-6-phosphate hydrolase (treC), were also found in the mutant strain YSD YN2 genome. Table 5 summarizes the PGP-related genes/gene clusters.

Conclusion

The *C. esculentus* L. endophyte *Franconibacter* sp. YSD YN2 exhibited strong salt tolerance and growth-promoting features. It also improved plant biomass and antioxidant capacity. Our results indicated that the *C. esculentus* L. endophyte might serve as a candidate growth-promoting agent for improving plant yield and can be used commercially. In addition, the use of the ARTP technology provided an effective method to improve the growth-promoting ability of this strain. Finally, the analysis of the mutant strain YSD YN2 whole genome contributed to understanding the genetic mechanisms related to growth promotion. This analysis also facilitated the development of such an endophyte as a microbial inoculum. To the best of our knowledge, only a few growth-promoting and salt-tolerant strains of *C. esculentus* L. endophytic bacteria have been identified until now.

Supplementary Information

The online version contains supplementary material available at https://doi.org/10.1186/s13213-021-01656-2.

Additional file 1: Table S1. Statistical table of gene function annotation of the mutant strain YSD YN2. **Figure S1.** GO annotation results of the mutant strain YSD YN2 genome. **Figure S2.** KEGG annotation results of the mutant strain YSD YN2 genome.

Additional file 2: Tables S2. CAZy annotation. **Table S3.** VFDB. **Table S4.** PHI. **Table S5.** Secretion System. **Table S6.** CARD. **Table S7.** Two components.

Acknowledgments

We thank Tong Yue for technical assistance. This work was supported by grants from the National Natural Science Foundation of China with Grant number 31801511, Science and Technology Commission of Shanghai Municipality (STCSM) for the Shanghai Agriculture Applied Technology Development Program with Grant number G20200201, Shanghai Natural Science Foundation with Grant number 19ZR1436800, Shanghai Sailing Program with Grant number 20YF1443000, Technology Support Project number KJZC202008, Shanghai Fresh Corn Technology System Project No.10 2021, the Shanghai Agricultural Science and Technology Innovation Action Plan (21N31900800), the Shanghai Academy of Agricultural Sciences (SAAS) with program for Excellent Research Team No. 2017 (B-07). Finally, we want to thank the anonymous reviewers since their comments are very constructive and helpful for the improvement of this work.

Authors' contributions

All authors contributed equally to the work. The first author is a PhD candidate and responsible for the data collections. XMT and YNH are the main supervisor and principal investigator for this research. JBW is an expert in genomic data analysis, and YFZ contributed partially to data analysis. SSW and JBW read the overview of the manuscript and data organization. YNH and XMT approved special funding related to the research work and publication. The authors read and approved the final manuscript.

Funding

This study was funded by the National Natural Science Foundation of China (31801511), the Shanghai Agricultural Science and Technology Innovation Action Plan (21N31900800), the Shanghai Agriculture Applied Technology Development Program (Grant No. G20200201), Shanghai Natural Science Foundation (No. 19ZR1436800), Shanghai Sailing Program (No. 20YF1443000), Technology Support Project (No. KJZC202008), Shanghai Fresh Corn Technology System Project (No.10 2021), and the SAAS Program for Excellent Research Team (No. 2017 (B-07)).

Availability of data and materials

Sequence data have been deposited into NCBI under BioProject PRJNA726370. The Fasta genome submission was under accession number CP074352-CP074353 (https://submit.ncbi.nlm.nih.gov).

Declarations

Ethics approval and consent to participate

This article does not contain any studies with human participants or animals performed by any authors. Informed consent was obtained from all individual participants included in the study.

Consent for publication

All authors agreed to participate and agreed on the submission.

Competing interests

The authors declare that they have no competing interests.

Author details

[1]School of Biotechnology, Jiangnan University, Wuxi 214122, China. [2]Biotechnology Research Institute Key Laboratory of Agricultural Genetics and Breeding, Shanghai Academy of Agricultural Sciences, Shanghai 201106, China. [3]Crops Ecological Environment Security Inspection and Supervision Center (Shanghai), Ministry of Agriculture and Rural Affairs, P.R.C., 2901 Beidi Road, Shanghai 201106, China. [4]School of Agriculture and Biology, Shanghai Jiao Tong University, Shanghai 200240, China.

Received: 2 July 2021 Accepted: 12 November 2021
Published online: 07 January 2022

References

Afridi MS, Amna S, Mahmood T, Salam A, Mukhtar T, Mehmood S, Ali J, Khatoon Z, Bibi M, Javed MT, Sultan T, Chaudhary HJ (2019) Induction of tolerance to salinity in wheat genotypes by plant growth promoting endophytes: involvement of ACC deaminase and antioxidant enzymes. Plant Physiol Bioch 13:569–577. https://doi.org/10.1016/j.plaphy.2019.03.041

Ahmad F, Ahmad I, Khan MS (2008) Screening of free-living rhizospheric bacteria for their multiple plant growth promoting activities. Microbiol Res 163(2):173–181

Arguelles-Arias A, Ongena M, Halimi B, Lara Y, Brans A, Joris B, Fickers P (2009) *Bacillus amyloliquefaciens* GA1 as a source of potent antibiotics and other secondary metabolites for biocontrol of plant pathogens. Microb Cell Fact 8:63

Bado S, Bazongo P, Son G, Kyaw MT, Bassolé IHN (2015, 2015) Physicochemical characteristics and composition of three morphotypes of *Cyperus esculentus* tubers and tuber oils. J Anal Methods Chem (2015-10-11), 2015(ID 673547)

Bairoch A, Apweiler R (2000) The SWISS-PROT protein sequence database and its supplement TrEMBL in 2000. Nucleic Acids Res 28(1):45

Bankevich A, Nurk S, Antipov D, Gurevich AA, Dvorkin M, Kulikov AS, Lesin VM, Nikolenko SI, Pham S, Prjibelski AD (2012) Spades: a new genome assembly algorithm and its applications to single-cell sequencing. J Comput Biol 19(5):455–477

Bélanger M, Burrows LL, Lam JS (1999) Functional analysis of genes responsible for the synthesis of the B-band O antigen of *Pseudomonas aeruginosa* serotype O6 lipopolysaccharide. Microbiology (Reading, England) 145(Pt 12):3505–3521. https://doi.org/10.1099/00221287-145-12-3505
Bertelli C, Laird MR, Williams KP (2017) IslandViewer 4: Expanded prediction of genomic islands for larger-scale datasets. Nucleic Acids Res 45(W1), W30–W35. https://doi.org/10.1093/nar/gkx343.
Besemer J, Borodovsky M (2005) GeneMark: web software for gene finding in prokaryotes, eukaryotes and viruses. Nucleic Acids Res 33(Web Server):W451–W454
Bidabadi SS, Mehralian M (2020) Seed bio-priming to improve germination, seedling growth and essential oil yield of *Dracocephalum kotschyi* Boiss, an endangered medicinal plant in Iran. Gesunde Pflanzen 72:17–27. https://doi.org/10.1007/s10343-019-00478-2
Bland C, Ramsey TL, Sabree F, Lowe M, Brown K, Kyrpides NC, Hugenholtz P (2007) CRISPR recognition tool (CRT): a tool for automatic detection of clustered regularly interspaced palindromic repeats. BMC Bioinformatics 8:209. https://doi.org/10.1186/1471-2105-8-209
Blin K, Wolf T, Chevrette MG, Lu X, Schwalen CJ, Kautsar SA, Medema MH (2017) AntiSMASH 4.0-improvements in chemistry prediction and gene cluster boundary identification. Nucleic Acids Res 45(W1):W36–W41
Bradford MM (1976) A rapid and sensitive method for the quantitation of microgram quantities of protein utilizing the principle of protein-dye binding. Anal Biochem 72:248–254
Brodmann A, Schuller A, Ludwig-Müller J, Aeschbacher R, Wiemken A, Boller T, Wingler A (2002) Induction of trehalase in Arabidopsis plants infected with the trehalose-producing pathogen *Plasmodiophora brassicae*. Mol Plant Microbe In 15(7):693–700. https://doi.org/10.1094/MPMI.2002.15.7.693
Cai L, Zheng SW, Shen YJ, Zheng GD, Liu HT, Wu ZY (2018) Complete genome sequence provides insights into the biodrying-related microbial function of *Bacillus thermoamylovorans* isolated from sewage sludge biodrying material. Bioresour Technol 260:141–149
Calvo P, Nelson L, Kloepper JW (2014) Agricultural uses of plant biostimulants. Plant Soil 383:3–41
Chan PP, Lowe TM (2019) tRNAscan-SE: searching for tRNA Genes in Genomic Sequences. Methods Mol Biol 1962:1–14
Chen L, Shi H, Heng JY, Wang DX, Bian K (2019) Antimicrobial, plant growth-promoting and genomic properties of the peanut endophyte *Bacillus velezensis* LDO2. Microbiol Res 218:41–48
Delcher AL, Bratke KA, Powers EC, Salzberg SL (2007) Identifying bacterial genes and endosymbiont DNA with GLIMMER. Bioinformatics 23(6):673–679
Delshadi S, Ebrahimi M, Shirmohammadi E (2017) Influence of plant-growth-promoting bacteria on germination, growth and nutrient uptake of *Onobrychis sativa* L., under drought stress. J Plant Interact 12(1):200–208. https://doi.org/10.1080/17429145.2017.1316527
Esfahani N, Mostajeran (2011) Rhizobial strain involvement in symbiosis efficiency of chickpea-rhizobia under drought stress: plant growth, nitrogen fixation and antioxidant enzyme activities. Acta Physiol Plant 33(4):1075–1083
Faino L, Seidl MF, Datema E, van den Berg GC, Janssen A, Wittenberg AH, Thomma BP (2015) Single-molecule real-time sequencing combined with optical mapping yields completely finished fungal genome. MBio 6:e00936–e00915
Fan X, Wu H, Li G, Yuan H, Zhang H, Li Y (2017) Improvement of uridine production of *Bacillus subtilis* by atmospheric and room temperature plasma mutagenesis and high-throughput screening. PLoS One 12(5):e0176545
Farías-Rodríguez R, Mellor RB, Arias C (1998) The accumulation of trehalose in nodules of several cultivars of common bean (*Phaseolus vulgaris*) and its correlation with resistance to drought stress. Physiol plantarum 102(3):353–359
Fincheira P, Quiroz A (2018) Microbial volatiles as plant growth inducers. Microbiol Res 208:63–75
Finn RD, Alex B, Jody C, Penelope C, Eberhardt RY, Eddy SR, Andreas H, Kirstie H, Liisa H, Jaina M (2014) Pfam: the protein families database. Nucleic Acids Res 42(D1):D222–D230
Fouts DE (2006) Phage_Finder: automated identification and classification of prophage regions in complete bacterial genome sequences. Nucleic Acids Res 34(20):5839–5851
Gao XL, Liu E, Yin YY, Yang LX, Huang QR, Chen S, Ho CT (2020) Enhancing activities of salt-tolerant proteases secreted by *Aspergillus oryzae* using atmospheric and room-temperature plasma mutagenesis. J Agric Food Chem 68:2757–2764
Han AW, Sandy M, Fishman B, Trindade-Silva AE, Soares CA, Distel DL, Butler A, Haygood MG (2013) Turnerbactin, a novel triscatecholate siderophore from the shipworm endosymbiont *Teredinibacter turnerae* T7901. PLoS One 8(10):e76151. https://doi.org/10.1371/journal.pone.0076151
He J, Qin J, Long L, Ma Y, Li H, Li K, Jiang X, Liu T, Polle A, Liang Z, Luo ZB (2011) Net cadmium flux and accumulation reveal tissue-specific oxidative stress and detoxification in *Populus* × *canescens*. Physiol Plantarum 143:50–63. https://doi.org/10.1111/j.1399-3054.2011.01487.x
Hmaeid N, Wali M, Metoui-Ben Mahmoud O, Pueyo JJ, Ghnaya T, Abdelly C (2019) Efficient rhizobacteria promote growth and alleviate NaCl-induced stress in the plant species *Sulla carnosa*. Appl Soil Ecol 133:104–113
Huygh W, Larridon I, Reynders M, Muasya AM, Govaerts R, Simpson DA, Goetghebeur P (2010) Nomenclature and typification of names of genera and subdivisions of genera in Cypereae (Cyperaceae): 1. Names of genera in the *Cyperus* clade. Taxon 59:1883–1890
Isidorov VA, Lech P, Żółciak A, Rusak M, Szczepaniak L (2008) Gas chromatographic–mass spectrometric investigation of metabolites from the needles and roots of pine seedlings at early stages of pathogenic fungi *Armillaria ostoyae* attack. Trees 22(4):531–542
Jensen LJ, Julien P, Kuhn M, Mering CV, Muller J, Doerks T, Bork P (2008) eggNOG: automated construction and annotation of orthologous groups of genes. Nucleic Acids Res 36(suppl 1):D250–D254
Jing SQ, Wang SS, Li Q, Zheng L, Yue L, Fan SL, Tao GJ (2016) Dynamic high pressure microfluidization-assisted extraction and bioactivities of *Cyperus esculentus* (C. *esculentus* L.) leaves flavonoids. Food Chem 192:319–327
Jing SQ, Wang SS, Zhong RM, Zhang JY, Wu JZ, Tu YX, Pu Y, Yan LJ (2020) Neuroprotection of *Cyperus esculentus* L. orientin against cerebral ischemia/reperfusion induced brain injury. Neural Regeneration Res 15(03):548–556
Kanehisa M, Goto S (2000) KEGG: Kyoto Encyclopedia of Genes and Genomes. Nucleic Acids Res 28(1):27–30
Kang SM, Radhakrishnan R, You YH, Joo GJ, Lee IJ, Lee KE, Kim JH (2014) Phosphate solubilizing *Bacillus megaterium* mj1212 regulates endogenous plant carbohydrates and amino acids contents to promote mustard plant growth. Indian J Microbiol 54:427–433
Kaya MD, Okcu G, Atak M, Cikli Y, Kolsarici O (2006) Seed treatments to overcome salt and drought stress during germination in sunflower (*Helianthus annuus* L.). Eur J Agron 24:291–296
Larridon I, Huygh W, Reynders M, Muasya AM, Govaerts R, Simpson DA, Goetghebeur P (2011) Nomenclature and typification of names of genera and subdivisions of genera in Cypereae (Cyperaceae): 2. Names of subdivisions of *Cyperus*. Taxon 60:868–884
Luo R, Liu B, Xie Y, Li Z, Huang W, Yuan J, He G, Chen Y, Pan Q, Liu Y, Tang J, Wu G, Zhang H, Wang J (2012) SOAPdenovo2: an empirically improved memory-efficient short-read de novo assembler. Gigascience 1:18
Mahmood A, Turgay OC, Farooq M, Hayat R (2016) Seed biopriming with plant growth promoting rhizobacteria: a review. FEMS Microbiol Ecol 92(8):1–14. https://doi.org/10.1093/femsec/fiw112
Morales-Cedeño LR, del Carmen Orozco-Mosqueda M, Loeza-Lara PD, Parra-Cota FI, de los Santos-Villalobos S, Santoyo G (2021) Plant growth-promoting bacterial endophytes as biocontrol agents of pre- and post-harvest diseases: fundamentals, methods of application and future perspectives. Microbiol Res. https://doi.org/10.1016/j.micres.2020.126612
Mukhtar S, Shahid I, Mehnaz S, Malik KA (2017) Assessment of two carrier materials for phosphate solubilizing biofertilizers and their effect on growth of wheat (*Triticum aestivum* L.). Microbiol Res 205:107–117
Nanjundan J, Ramasamy R, Uthandi S, Ponnusamy M (2019) Antimicrobial activity and spectroscopic characterization of surfactin class of lipopeptides from *Bacillus amyloliquefaciens* SR1. Microb Pathogenesis 128:374–380
Ntukidem VE, Ukwo PS, Udoh IE, Umoinyang EU (2019) Influence of different pretreatments on the nutritional and organoleptic properties of vegetable milk produced locally from tiger-nut (*Cyperus esculentus*) tubers. IOSR-JESTFT 13(6):55–61
Nyarko HD, Daniel NAT, Yaw A (2011) Assessment of microbiological safety of tiger nuts (*Cyperus esculentus* L.) in the Cape Coast Metropolis of Ghana. Arch Appl Sci Res 3(6):257–262
Ottenheim C, Nawrath M, Wu JC (2018) Microbial mutagenesis by atmospheric and room-temperature plasma (ARTP): the latest development. Bioresour Bioprocess 5(1):1–12

Pan S, Rasul F, Li W, Tian H, Mo Z, Duan M, Tang X (2013) Roles of plant growth regulators on yield, grain qualities and antioxidant enzyme activities in super hybrid rice (*Oryza sativa* L.). Rice (N Y) 6(1):9. https://doi.org/10.1186/1939-8433-6-9
Ramesh A, Sharma SK, Sharma MP, Yadav N, Joshi OP (2014) Inoculation of zinc solubilizing *Bacillus aryabhattai* strains for improved growth, mobilization and biofortification of zinc in soybean and wheat cultivated in vertisols of central India. Appl Soil Ecol 73:87–96
Rowse HR (1995) Drum priming-a non-osmotic method of priming seeds. Seed Sci Technol 24:281–294
Ryu CM, Farag MA, Hu CH, Reddy MS, Wei HX, Pare PW, Kloepper JW (2003) Bacterial volatiles promote growth in Arabidopsis. Proc Natl Acad Sci USA 100:4927–4932
Santoyo G, Moreno-Hagelsieb G, Orozco-Mosqueda M, Glick B (2016) Plant growth-promoting bacterial endophytes. Microbiol Res 83:92–99
Schwyn B, Neilands JB (1987) Universal chemical assay for the detection and determination of siderophores. Anal Biochem 160:47–56
Shi L, Thinn NT, Ge B, Zhao W, Liu B, Cui H, Zhang K (2018) Antifungal and plant growth-promoting activities of *Streptomyces roseoflavus* strain NKZ-259. Biol Control 125:57–64. https://doi.org/10.1016/j.biocontrol.2018.06.012
Shu L, Si X, Yang X, Ma W, Sun J, Zhang J, Xue X, Wang D, Gao Q (2020) Enhancement of acid protease activity of *Aspergillus oryzae* using atmospheric and room temperature plasma. Front Microbiol 11:1418
Stella M, Halimi M (2015) Gluconic acid production by bacteria to liberate phosphorus from insoluble phosphate complexes. J Trop Agric Food Sci 43:41–45
Strobel G, Stierle A, Stierle D, Hess WM (1993) Taxomyces andreanae, a proposed new taxon for a *Bulbilliferous hyphomycete* associated with Pacific yew (*Taxus brevifolia*). Mycotaxon (USA) 47(71):71–80
Suárez R, Wong A, Ramírez M, Barraza A, Orozco MDC, Cevallos MA, Lara M, Hernández G, Iturriaga G (2008) Improvement of drought tolerance and grain yield in common bean by overexpressing trehalose-6-phosphate synthase in rhizobia. Mol Plant Microbe Interact 21(7):958–966
Tamura K, Stecher G, Peterson D, Filipski A, Kumar S (2013) MEGA6: molecular evolutionary genetics analysis version 6.0. Mol Biol Evol 30(12):2725–2729
Tang YJ, Martin HG, Dehal PS, Deutschbauer AM, Llora X, Meadows A, Arkin A, Keasling JD (2009) Metabolic flux analysis of Shewanella spp. reveals evolutionary robustness in central carbon metabolism. Biotechnol Bioeng 102(4):1161–1169
Ullah I, Waqas M, Khan MA (2017) Exogenous ascorbic acid mitigates flood stress damages of *Vigna angularis*. Appl Biol Chem 60:603–614
Vinale F, Sivasithamparam K, Ghisalberti E, Marra R, Woo S, Lorito M (2007) Trichoderma-plant-pathogen interactions. Soil Biol Biochem 40:1–10
Wang W, Wu Z, He Y, Huang Y, Li X, Ye BC (2018) Plant growth promotion and alleviation of salinity stress in *Capsicum annuum* L. by *Bacillus* isolated from saline soil in Xinjiang. Ecotoxicol Environ Saf 164:520–529
Wilson MK, Abergel RJ, Raymond KN, Arceneaux JEL, Byers BR (2006) Siderophores of *Bacillus anthracis*, *Bacillus cereus*, and *Bacillus thuringiensis*. Biochem Biophys Res Commun 348:320–325
Yaghoubi Khanghahi M, Pirdashti H, Rahimian H, Nematzadeh G, Ghajar Sepanlou M (2018) Potassium solubilising bacteria (KSB) isolated from rice paddy soil: from isolation, identification to K use efficiency. Symbiosis 76:13–23. https://doi.org/10.1007/s13199-017-0533-0
Yang L, Zhou N, Tian Y (2019) Characterization and application of dextranase produced by *Chaetomium globosum* mutant through combined application of atmospheric and room temperature plasma and ethyl methyl sulfone. Process Biochem 85:116–124
Zhuang Y, Jiang GL, Zhu MJ (2020) Atmospheric and room temperature plasma mutagenesis and astaxanthin production from sugarcane bagasse hydrolysate by *Phaffia rhodozyma* mutant Y1. Process Biochem 91:330–338

Publisher's Note